RESEARCH ARTICLE

• Arch Hyg Sci 2021;10(1):86-96
• Journal Homepage: http://jhygiene.muq.ac.ir

Kinetic Studies on Penicillin G Removal from Aqueous Environments by Cupric Oxide Nanoparticles

Shahin Ahmadi[a*], Chinenye Adaobi Igwegbe[b]

[a] Department of Environmental Health, Zabol University of Medical Sciences, Zabol, Iran
[b] Department of Chemical Engineering, Nnamdi Azikiwe University, Awka, Nigeria

***Correspondence** should be addressed to Dr Shahin Ahmadi, Email: sh.ahmadi398@gmail.com

A-R-T-I-C-L-EI-N-F-O

Article Notes:
Received: Jun 09, 2018
Received in revised form: Oct 12, 2019
Accepted: Jan 11, 2020
Available Online: Jan 23, 2021

Keywords:
Adsorption
Aqueous solutions
Cupric oxide nanoparticles
Kinetics
Penicillin G

A-B-S-T-R-A-C-T

Background & Aims of the Study: Antibiotics are pharmaceutical compounds which are stable in the environment and their discharge without treatment can cause pollution of the environment. The current study aimed to assess the efficicacy of cupric oxide nanoparticles (CuO-NPs) as another kind of adsorbent for the removal of penicillin G (PG) from its aqueous media, as well as kinetic analysis of PG removal.
Materials and Methods: In the present study, batch experiments were conducted on a laboratory scale. During the process of adsorption, the optimum conditions (including contact time, initial PG concentration, initial pH, and dosage of CuO-NPs) were determined. The sorption data was fitted into the pseudo-first-order (PFO), pseudo-second-order (PSO), Bhattacharya-Venkobachar, and intraparticle diffusion models.
Results: As evidenced by the obtained results, the maximum removal efficiency for PG (83%) was measured at pH 6, CuO-NPs dose of 1 g/L, PG concentration of 25 mg/L and the contact time of 60 min with adsorption capacity (q_e) of 15 mg/g. The sorption data were more adequately fitted into the PSO model.
Conclusion: Based on the findings of the present study, CuO-NPs are efficient for PG removal; therefore, they can be employed for PG reduction from the environment.

Please cite this article as: Ahmadi S, Igwegbe CA. Kinetic Studies on Penicillin G Removal from Aqueous Environments by Cupric Oxide Nanoparticles. Arch Hyg Sci 2021;10(1):86-96

Background

Excessive use of antibiotics and their disposal into the environment poses a serious threat to public health (1). Penicillin G (PG) injection is used to treat and prevent a wide range of infections caused by bacteria, and pH-heat sensitivity has been reported for this beta-lactam antibiotic (2). It spontaneously dissolves in water, as well as isotonic sodium chloride and dextrose solutions (3, 4). Different methods, including electrolysis (5, 6), adsorption (7, 8), oxidation (9), biodegradation (10), and dissolved air flotation (1, 2), are used to remove PG from contaminated water. The adsorption process has an extensive application in industries for the elimination of organic pollutants (11). Granular activated carbons are widely utilized adsorbing materials; nonetheless, they are hardly regenerated (12). Nanoparticles (NPs) are tiny materials sized within 1-100 nanometers (nm). Today NPs have a widespread application in various

industries and professions, including textiles, paint, and diagnosis of diseases. Therefore, the research focus has now shifted towards nanotechnology and its development. NPs can be perfused into the polluted environment by pressure and/or under gravity owing to their very small size. Moreover, they remain in the solution as a suspension under certain conditions for a long time and flow through the water to have enough opportunity to decontaminate the pollutant (13).

Copper oxide nanoparticles (CuO-NPs) are used as a catalyst with high efficiency due to their high efficiency and quantum size effect (7). The present study aimed to assess the efficiency of CuO-NPs in the removal of PG from aqueous solution. To determine the optimum conditions, the effects of operational factors: the adsorbent (CuO-NPs) dosage, contact time, as well as pH and initial concentration of PG were examined. On a final note, the kinetic adsorption models were utilized to fit the experimental data.

Materials & Methods

The cupric oxide nanoparticles (CuO-NPs) obtained from Sigma Company has the following characteristics: size: 15-20 nm and purity: 99%. Penicillin G (PG) with a molecular weight of 372.48 g/mol, purity higher than 99%, and molecular formulae of $C_{16}H_{17}KN_2O_4S$ was provided by Sigma-Aldrich. Different PG concentrations used for the study were prepared from a 1000 mg/L stock solution using distilled water. The structure of PG is displayed in Figure 1.

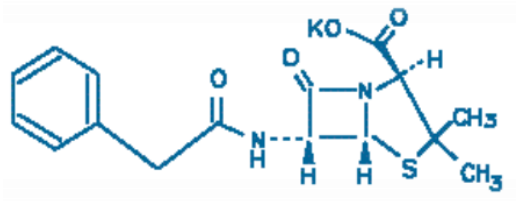

Figure 1) The chemical structure of penicillin G

For the adsorption process experiments, the impact of various factors, namely pH (3, 5, 7, 9, 11), contact time (15, 30, 45, 60, 75, 90, 120 min), pollutant concentration (10, 25, 50,100,150, 200 mg/L) and adsorbent dose (0.1, 0.3, 0.5, 0.7, 0.9, 1 g/L) was assessed. A shaker of 150 rpm was used to create optimal conditions. The adsorbent was added to each 1 L of water sample containing PG at various concentrations. The solutions were agitated using an orbital shaker (with a speed of 150 rpm) for a specified time to reach equilibrium. Subsequently, the samples were eliminated, and the supernatant solution was filtered through Whatman filter paper no. 41. The pH adjustments of the water samples were performed by the addition of hydrochloric acid 0.1 N or 0.1 N sodium hydroxide solutions. A UV-visible recording spectrophotometer (Shimadzu Model: LUV-100A) was used to analyze the initial PG concentration and final PG concentration remaining in solutions. The concentrations of PG were determined at a wavelength of maximum absorbance (λ_{max}) of 248 nm (1, 14).

The PG removal efficiency (*%R*) of the studied parameters was calculated using the following formula (15):

$$\%R = \frac{(C_0 - C_f)}{C_0} 100 \quad [1]$$

where C_0 and C_f are the initial and final PG concentrations, respectively.

The amount of PG adsorbed by CuO-NPs, q_e (mg/g) was calculated using the following mass balance relationship stated as Equation [2](16):

$$q_e = \frac{(C_0 - C_e)V}{M} \quad [2]$$

where *M* is the weight of CuO-NPs used (g), and *V* is the volume of the PG solution treated (L). C_0 and C_e are the initial and final equilibrium liquid-phase concentrations of PG

(mg/g), respectively.

Adsorption kinetics

The rate of adsorption and the potential rate-controlling steps are assessed by kinetic models. The pseudo-first-order (PFO) rate equation is expressed as Equation [3](17):

$$Log(q_e - q_t) = Log(q_e) - \frac{k_1}{2.303}t \quad [3]$$

where qe and qt are the amounts of PG adsorbed (mg/g) at equilibrium and at time t (min), respectively, and k1 is the PFO rate constant of adsorption (min−1).

The pseudo-second-order (PSO) rate equation is stated as Equation [4](18, 19).

$$\frac{t}{q_t} = \frac{1}{k_2 q^2} + \frac{t}{q\ e} \quad [4]$$

where k2 is the PSO rate constant (g mg−1min−1), qt and qe are the amounts of PG adsorbed on the CuO-NPs (mg/g) at equilibrium and at time t, respectively.

The adsorption of PG on CuO-NPs may be controlled by intraparticle diffusion or penetration process. Its mathematical model is expressed as Equation [5](20, 21):

$$q_t = K_{pi}t^{0.5} + c \quad [5]$$

where c is a constant, Kpi is the intraparticle diffusion rate constant (mg/g min1/2), and qt is the amount adsorbed (mg/g) at time t (min).

Bhattacharya and Venkobachar kinetic equation is stated as Equation [6](22):

$$Log(1 - U_{(T)}) = \frac{K_1}{2.303}t \quad [6]$$

where Ci and Ct = concentration of PG at time zero and time t, respectively (mg/L). Moreover, qe and qt = amount of PG adsorbed at equilibrium time and time t, respectively (mg/g).

where Ce = equilibrium dye concentration (mg/L), and k1 = first-order adsorption rate constant (min-l).

Results

Scanning electron microscopy (SEM) image of Copper oxide nanoparticles

The scanning electron microscopy (SEM) method was applied to measure the specific surface area of the nanoparticles. SEM has been extensively used to characterize the surface morphology and major physical advantage of the adsorbent surface. The specific surface area of CuO-NPs was measured as 20 m2/g. Figure 2 (SEM image of 300x and 800x) demonstrates that the CuO-NPs appear spongy in nature.

Influence of initial pH

The effect of different pH (2 to 12) on the adsorption of PG on CuO-NPs is displayed in Figure 3. The removal efficiency of PG was elevated by increasing the pH values from 2 to 6, while a pH higher than 6 reduced the removal efficiency. The removal efficiency increased

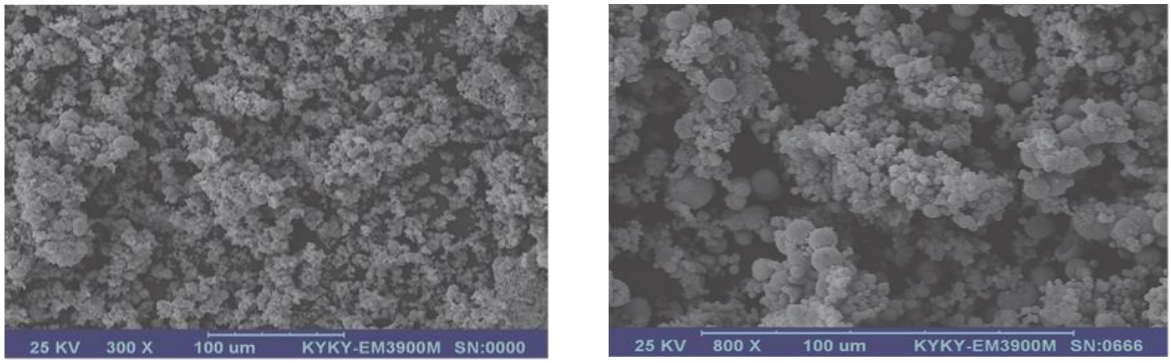

Figure 2) Scanning electron microscopy image of Copper oxide nanoparticles

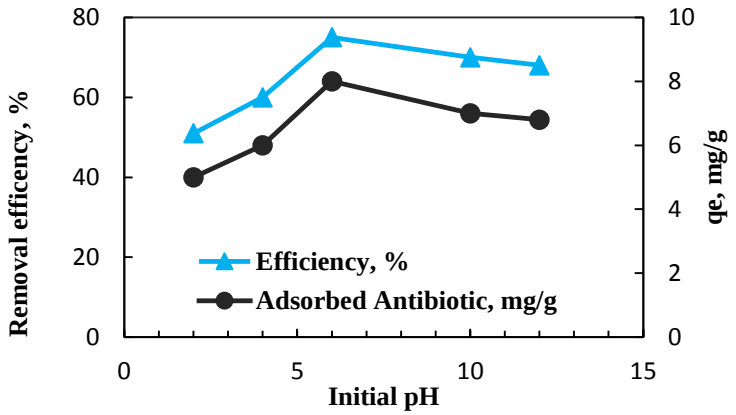

Figure 3) Effect of pH on the removal of penicillin G onto cupric oxide nanoparticles (Time: 60 min, CuO-NPs dosage: 0.9 g/L, PG concentration: 50 mg/L)

from 51 to 75 % when pH was increased from 2 to 6. The optimal pH for the adsorption of PG on CuO-NPs was obtained at 6.

Influence of contact time and initial penicillin concentration

To assess the impact of contact time and initial PG concentration on the adsorption process, the initial concentration of PG varied from 25 to 100 mg/L at the optimum pH, the contact time of 60 min, and the CuO-NPs dose of 0.1 g/L. As illustrated in Figure 4, the initial concentration of 25 mg/L resulted in optimum efficiency removal.

The impact of contact time on percentage removal of PG onto CuO-NPs at a constant initial concentration of 25 mg/L, optimum pH, and the optimum CuO-NPs dosage is demonstrated in Figure 4. The adsorption of PG on CuO-NPs was rapid in the first 60 min.

Effect of cupric oxide nanoparticles dosage

As indicated in Figure 5, the adsorbent dose exerts a significant impact on the amount of adsorbed adsorbate. The impact of CuO-NPs dose on the elimination of PG was investigated by varying the dose of CuO-NPs from 0.1-1 g/L. The removal efficiency increased from 65-83% when the CuO-NPs dosage was raised from 0.1 to 1 g/L at the PG concentration of 25 mg/L. On the other hand, the biosorption capacity (qe) of PG on CuO-NPs decreased from 15 to 4.15 mg/g when CuO-NPs dosage increased from 0.1 to 1 g/L.

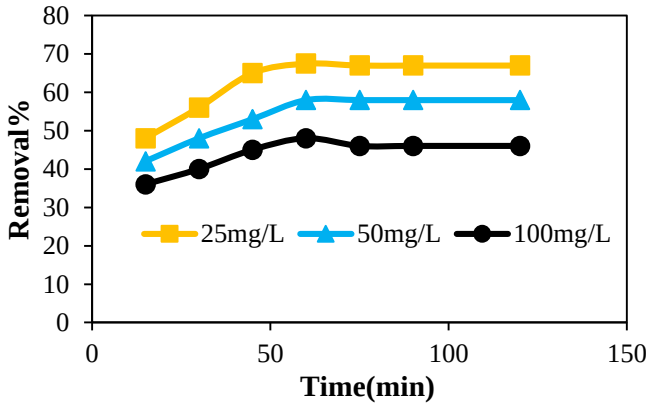

Figure 4) Effect of time on the removal of penicillin G onto cupric oxide nanoparticles (pH: 6, CuO-NPs dosage: 0.1 g/L)

Adsorption kinetics

The results and correlation coefficients for Kinetic Model are presented in Table 1, and Figure 6-9.

Values of k1 (depicted in Table 1) were evaluated from the slopes of the log plots of (qe − qt) versus (t) for 25, 50, and 100 mg/L concentrations (Figure 6).

The parameters, k2, and qe (illustrated in Table 1) were determined from the intercepts and slopes of the plots of t/qt versus t, respectively, for 25, 50, and 100 mg/L

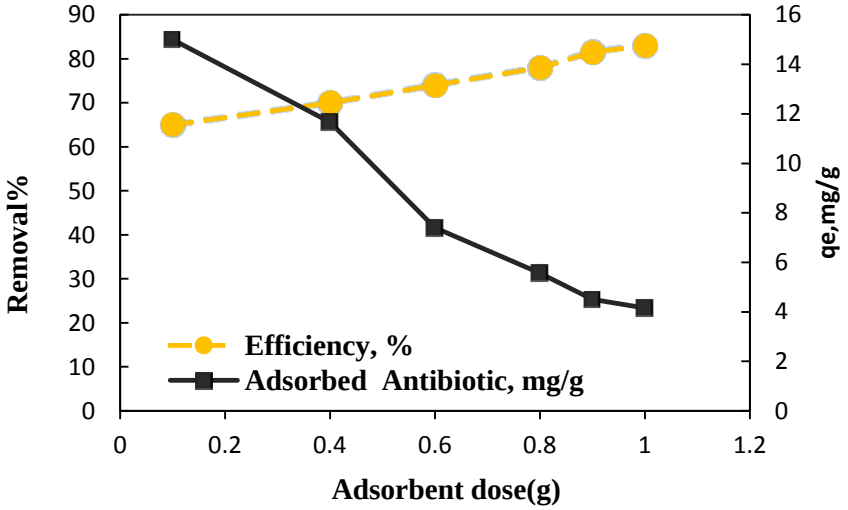

Figure 5) The effect of CuO-NPs dosage on the percentage removal of penicillin G onto cupric oxide nanoparticles (Time: 60 min, pH: 6, penicillin G concentration: 25 mg/L)

Table 1) Kinetic results for adsorption of penicillin G on cupric oxide nanoparticles

Initial PG concentration (mg/L)	PFO			PSO			Intraparticle diffusion			Bhattacharya - Venkobachar	
	q_e	k_1	R^2	q_e	k_2	R^2	c	K_{pi}	R^2	K_B	R^2
25	18.3	0.07	0.93	17.85	0.01	0.9963	10.56	0.67	0.738	0.17	0.9183
50	14.6	0.04	0.99	31.15	0.005	0.9977	17.79	1.19	0.821	0.086	0.9925
100	73.5	0.08	0.68	48.3	0.005	0.9975	33.04	1.43	0.664	0.177	0.9107

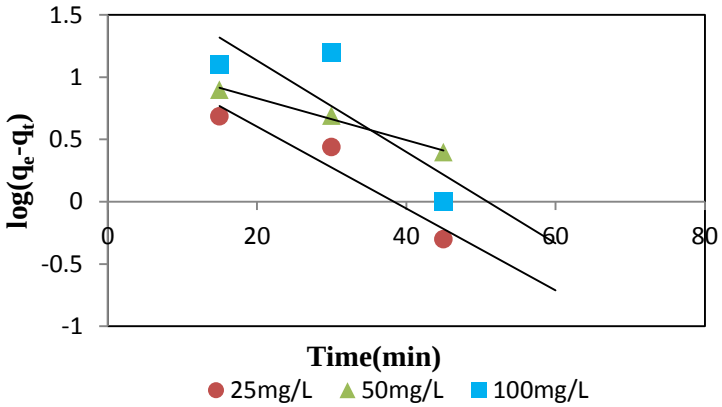

Figure 6) PFO plot of penicillin G adsorption onto cupric oxide nanoparticles

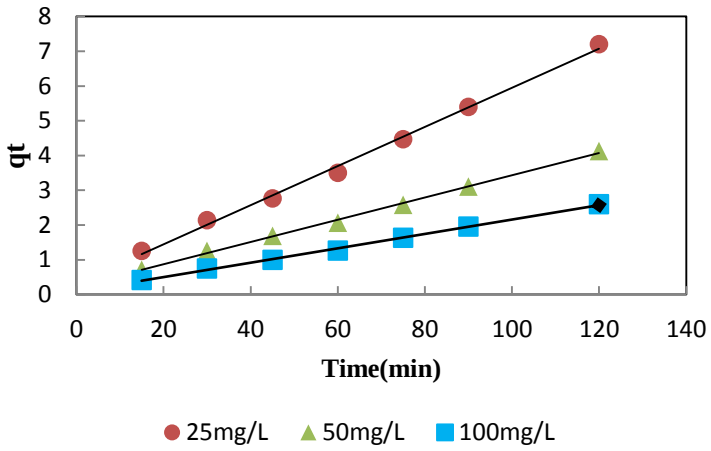

Figure 7) PSO plot of penicillin G sorption onto cupric oxide nanoparticles

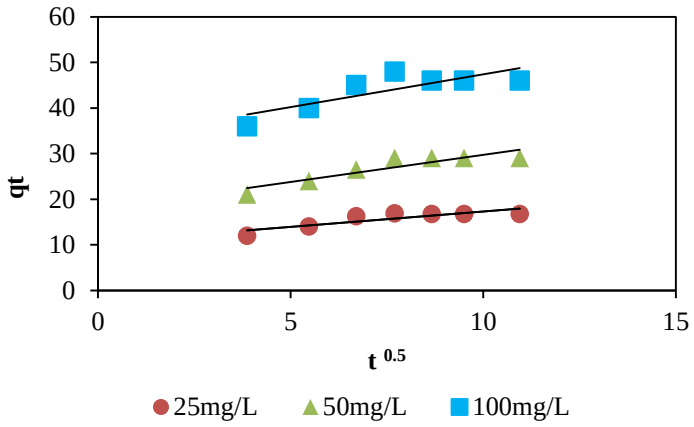

Figure 8) Intraparticle diffusion plot of penicillin G adsorption onto cupric oxide nanoparticles

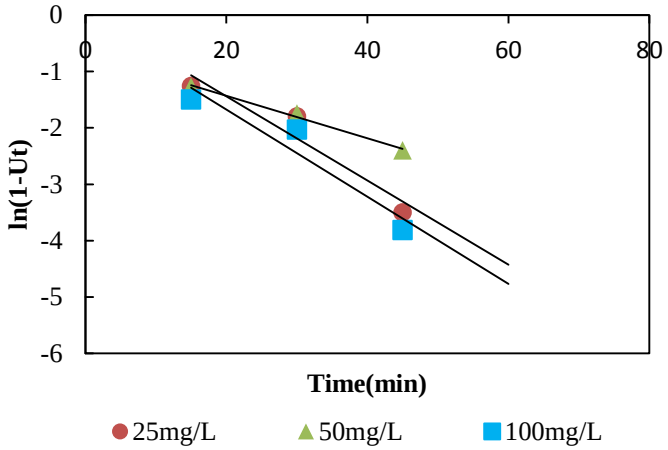

Figure 9) Bhattacharya -Venkobachar plot of penicillin G adsorption onto cupric oxide nanoparticles

concentrations (Figure 7).

The Kpi and c values (illustrated in Table 1) were estimated from the slopes and intercepts of linear plots of qt against t0.5, respectively for 25, 50, and 100 mg/L concentrations (Figure 8).

The linear plots of In (1-U(T)) versus t (Figure 9) were used to obtain the constant KB at different temperatures (Table 1).

By comparing the correlation coefficients R2, it can be seen that the experimental equilibrium sorption data are better described by the pseudo second-order model than by the other models.

Discussion

Large pores can be detected on the NPs pointing to the presence of adsorption sites on the adsorbent for PG removal. This will also lead to a high level of contact with the adsorbate (23, 24).

Solution pH is a key controlling parameter affecting the adsorption process. The anionic and cationic nature of the solution due to the competition between the ions of OH– and H+ with the adsorbate exerts a significant impact on the process of adsorbate removal on an adsorbent (24).

The increased rate of removal efficiency at pH of 6 is related to the point of zero charge and pKa of the CuO-NPs and PG, respectively. The point of zero charge is defined as the pH at which the net charge of the total particle surface is equal to zero (25). The PG pKa was reported as 2.75, and the pHzpc of CuO-NPs was equal to 9.4. The adsorbent had a positive charge at pH less than the pHzpc value. PG took a carboxylic agent (-COOH) in acidic pH, and in pKa less than 2.75, the carboxyl group transformed to carboxylate charge; therefore, the removal efficiency increased (26). At pH within 7-11, the OH- ions decreased resulting in a marked increase in competition between them and anions. The removal efficiency decreased as the result of the repulsive force of negative charges of adsorbent and COO- anions (27).

The PG reduction decreased with an increase in initial PG concentration. As the adsorption process progressed with higher dye concentration, the adsorbent surface was easily saturated by PG particles (28).

By increasing the time to 60 min, as the optimum time, the collision of the nanoparticles and PG increased and resulted in enhanced adsorption cross-section and efficiency (29-31). The reduction efficiency of PG on CuO-NPs was decreased by increasing the contact time above the optimum time (60 min) to 120 min. It can result from the existence of the desensitization (reversible) phenomenon (31, 32).

This can be attributed to the increase in adsorption sites with more nanoparticles resulting in a marked increase in adsorption capacity (33). The decrease in the adsorption capacity is also ascribed to active adsorption sites which are unsaturated during the process of PG removal on CuO-NPs (25, 34).

The kinetic results and the correlation coefficients (R2) for the kinetic models are listed in Table 1. Based on the obtained results (Table 1 and Figures 6-9), the present study (the adsorption of PG on CuO-NPs) fitted well with the PSO model. R2 is the rationale for choosing the PSO kinetic adsorption model as the appropriate model (R2>0.99) since this parameter is higher for this model, compared to other adsorption kinetic models. This is indicative of the predominance of the PSO model mechanism suggesting that R2 values for the PSO kinetic model are greater than 0.99 which is followed by the uptake process. This also denotes that the adsorption of PG on CuO-NPs is controlled by chemisorptions (22). The intraparticle diffusion is not a suitable controlling factor in determining the kinetics of the adsorption process since the c values were not close to the

origin and the values of R2 (Table) were not high (35, 36). A similar observation was made by Nourmoradi et al. (37) for PG removal on modified montmorillonite.

The adsorption capacities (qe) and removal efficiencies (%R) of PG removal using various adsorbents are listed in Table 2. Table 2 shows that CuO-NPs can be efficiently be used for the removal of PG from water containing PG, in comparison with other materials.

Table 2) Comparison of cupric oxide nanoparticles with other materials for the adsorptive removal of penicillin G

Sorbent material	Maximum q_e or *%R*	Conditions	Kinetic model tested	Reference
Single-walled nanotubes (SWCNT)	q_e = 141 mg/g *%R* = 68.25%	pH: 5 SWCNT dosage: 0.8 g/L Reaction time: 105 min PG concentration: 50 mg/L Working temperature: 10±2^{0}C Agitation speed: 300 rpm Volume of solution: 100 mL	-PFO (R^2=0.991) -PSO (R^2= 0.988)	(38)
Magnesium oxide (MgO) nanoparticles	q_e = 25.66 mg/g *%R* = 74.97%	pH: 3 nanoparticles dose: 1.5 g/L Reaction time: 60 min PG concentration:50 mg/L Working temperature: 298± 2 K Agitation speed: 180 rpm Volume of solution:100 mL	-	(39)
Cationic surfactant modified montmorillonite	q_e = 88.5 mg/g	pH: 9 Adsorbent mass: 0.1 g Reaction time: 60 min PG concentration: 150 mg/L Working temperature: 35±2^{0}C Agitation speed: 250 rpm Volume of solution: 100 mL Surfactant loading = 150%	-PFO (R^2= 0.489) -PSO (R^2= 0.999) -Intraparticle diffusion (R^2=0.491)	(37)
Multi-walled carbon nanotubes (MWCNT)	q_e = 119 mg/g *%R* = 56.37%	pH: 5 MWCNT dosage: 0.8 g/L Reaction time: 105 min PG concentration: 50 mg/L Working temperature: 10±2^{0}C Agitation speed: 300 rpm Volume of solution: 100 mL	-PFO (R^2= 0.156) -PSO (R^2=0.994)	(38)
Cupric oxide nanoparticles (CuO NPs)	q_e = 15 mg/g *%R* = 83 %	pH: 6 CuO-NPs dosage: 1 g/L Reaction time: 60 min PG concentration: 25 mg/L Working temperature: 30±2^{0}C Agitation speed: 150 rpm Volume of solution treated: 1 L	-PFO (R^2=0.68-0.99) -PSO (R^2=0.9963-0.9977) -Intraparticle diffusion (R^2=0.664-0.821) -Bhattacharya–Venkobachar (R^2=0.9107-0.9925)	This study

Conclusion

The present study assessed the adsorption of PG onto CuO-NPs. Based on the obtained results, CuO-NPs can be used as an alternative adsorbent for the removal of PG from its aqueous solution; with the CuO-NPs dosage of 1 g/L, PG concentration of 25 mg/L pH of 6 and contact time of 60 min, the optimum removal of 83% and adsorption capacity of 15 mg/g were attained. Consequently, PG adsorption by CuO-NPs fitted the pseudo-second-order model (suggesting chemical adsorption process) with a higher correlation coefficient (R^2 > 0.99), compared to that of pseudo-first-order, intraparticle diffusion, and Bhattacharya-Venkobachar models. Moreover, the best fit model for the experimental data was the Bhattacharya-Venkobachar and pseudo-first-order models.

Footnotes

Acknowledgements

The authors' deepest appreciation goes to the laboratory staff of Zabol University of Medical Sciences for their financial support and collaboration in this research project.

Funding

The current study was conducted with the financial and spiritual support of the Research Center of Zabol University of Medical Sciences.

Conflict of Interest

The authors state that they do not have any competing financial interests or personal connections that might have influenced the work presented in the paper.

References

1. Ahmadi S, Mostafapour FK. Survey of efficiency of dissolved air flotation in removal penicillin G potassium from aqueous solutions. J Pharm Res Int 2017;15(3):1-11. Link
2. Kord Mostafapour F, Ahmadi S, Balarak DA, Rahdar SO. Comparison of dissolved air flotation process Function for aniline and penicillin G removal from aqueous solutions. Avicenna J Clin Med 2017; 23(4):360-9. Link
3. Dehghani M, Nasseri S, Ahmadi M, Samaei MR, Anushiravani R. Removal of penicillin G from aqueous phase by Fe^{+3}-TiO_2/UV-A process. J Environ Health Sci Eng 2014;12(1):2-7. PMID: 24598354
4. Mostafaloo R, Yari AR, Mohammadi MJ, Khaniabadi YO, Asadi-Ghalhari M. Optimization of the electrocoagulation process on the effectiveness of removal of Cefixime antibiotic from aqueous solutions. Desalin Water Treat 2019;144:138-44. Link
5. Peterson JW, Petrasky LJ, Seymour MD, Burkhart RS, Schuiling AB. Adsorption and breakdown of penicillin antibiotic in the presence of titanium oxide nanoparticles in water. Chemosphere 2012;87:911-7. PMID: 22342282
6. Homen V, Santos L. Degradation and removal methods of antibiotics from aqueous matrices--a review. J Environ Manage 2011;92(10):2304-47. PMID: 21680081
7. Ahmadi S, Banach A, Mostafapour FK, Balarak D. Study survey of cupric oxide nanoparticles in removal efficiency of ciprofloxacin antibiotic. Desalin Water Treat 2017; 89:297-303. Link
8. Ahmadi S, Mohammadi L, Igwegbe CA, Rahdar S, Banach AM. Application of response surface methodology in the degradation of Reactive Blue 19 using H_2O_2/MgO nanoparticles advanced oxidation process. Int J Ind Chem 2018;9(3):241-53. Link
9. Martinez JL. Environmental pollution by antibiotics and by antibiotic resistance determinants. Environ Pollut 2009;157(11):2893-902. PMID: 19560847
10. Watkinson AJ, Murby EJ, Costanzo SD. Removal of antibiotics in conventional and advanced wastewater treatment: implications for environmental discharge and wastewater recycling. Water Res 2007; 41(18):4164-76. PMID: 1752445
11. Ahmadi S, Kord Mostafapoor F. Adsorptive removal of Bisphenol A from aqueous solutions by Pistacia atlantica: isotherm and kinetic studies. Pharm Chem J 2017;4(2):1-8. Link

12. Ahmadi S, Kord Mostafapour F. Adsorptive removal of aniline from aqueous solutions by Pistaciaatlantica (Baneh) shells: isotherm and kinetic studies. J Sci Technol Environ Inform 2017;5(1):327-35. Link
13. Carabineiro SA, Thavorn-Amornsri T, Pereira MF, Serp P, Figueiredo JL. Comparison between activated carbon, carbon xerogel and carbon nanotubes for the adsorption of the antibiotic ciprofloxacin. Catal Today 2012;186(1):29-34. Link
14. Rahdar S, Igwegbe CA, Rahdar A, Ahmadi S. Efficiency of sono-nano-catalytic process of magnesium oxide nano particle in removal of penicillin G from aqueous solution. Desalin Water Treat 2018;106:330-5. Link
15. Rahdar A, Ahmadi S, Fu J, Rahdar S. Iron oxide nanoparticle preparation and its use for the removal of fluoride from aqueous solution: application of isotherm, kinetic, and thermodynamics. Desalin Water Treat 2019;137:174-82. Link
16. Rahdar A, Rahdar S, Ahmadi S, Fu J. Adsorption of ciprofloxacin from aqueous environment by using synthesized nanoceria. Ecol Chem Eng 2019; 26(2):299-311. Link
17. Banerjee S, Chattopadhyaya MC. Adsorption characteristics for the removal of a toxic dye, tartrazine from aqueous solutions by a low cost agricultural by-product. Arabian J Chem 2017; 10:S1629-38. Link
18. Ahmadi S, Rahdar A, Randar S, Igwegbe CA. Removal of Remazol Black B from aqueous solution using P-gamma-Fe2O3 nanoparticles: synthesis, physical characterization, isotherm, kinetic and thermodynamic studies. Desalin Water Treat 2019; 152:401-10. Link
19. Venkatesha TG, Nayaka YA, Chethana BK. Adsorption of ponceau S from aqueous solution by MgO nanoparticles. Appl Surf Sci 2013;276:620-7. Link
20. Bazrafshan E, Ahmadi S. Removal COD of landfill leachate using coagulation and activated tea waste (ZnCLR2R) adsorption. Int J Innov Sci Eng Technol 2017;4(4):339-47. Link
21. Ahmadi S, Bazrafshan E, Kord Mostafapoor F. Treatment of landfill leachate using a combined Coagulation and modify bentonite adsorption processes. J Sci Eng Res 2017;4(2):58-64. Link
22. Sarvani R, Damani E, Ahmadi S. Adsorption isotherm and kinetics study: removal of phenol using adsorption onto modified pistacia mutica shells. Iran J Health Sci 2018;6(1):33-42. Link
23. Samadi MT, Kashitarash EZ, Ahangari F, Ahmadi S, Jafari SJ. Nickel removal from aqueous environments using carbon nanotubes. Water Wastewater 2012; 24(2):38-44. Link
24. Peterson JW, Petrasky LJ, Seymour MD, Burkhart RS, Schuiling AB. Adsorption and breakdown of penicillin antibiotics in the presence of titanium oxide nanoparticles in water. Chemosphere 2012;87(8):911-7. PMID: 22342282
25. Ahmadi S, Igwegbe CA, Rahdar S, Asadi Z. The survey of application of the linear and nonlinear kinetic models for the adsorption of nickel (II) by modified multi-walled carbon nanotubes. Appl Water Sci 2019;9(4):98. Link
26. Stafiej A, Pyrzynska K. Solid phase extraction of metal ions using carbon nanotubes. Microchem J 2008;89(1):29-33. Link
27. Rahdar S, Ahmadi S. Removal of phenol and aniline from aqueous solutions by using adsorption on to pistacia terebinthus, study of adsorption isotherm and kinetics. J Health Res Community 2017;2(4):35-45. Link
28. Rhdar S, Shikh L, Ahmadi S. Removal of reactive blue 19 dye using a combined sonochemical and Modified Pistachio Shell adsorption processes from aqueous solutions. Iran J Health Sci 2018;6(3):8-20. Link
29. Ahmadi S, Mostafapour FK, Bazrafshan E. Removal of aniline and from aqueous solutions by coagulation/flocculation–flotation. Chem Sci Int J 2017;18(3):1-10. Link
30. Ho YS, McKay G. Pseudo-second order model for sorption processes. Proc Biochem 1999;34(5):451-65. Link
31. Ahmadi S, Igwegbe CA. Adsorptive removal of phenol and aniline by modified bentonite: adsorption isotherm and kinetics study. Appl Water Sci 2018;8(6):170. Link
32. Ahmadi S, Rahdar S, Igwegbe CA, Rahdar A, Shafighi N, Sadeghfar F. Data on the removal of fluoride from aqueous solutions using synthesized P/γ-Fe_2O_3 nanoparticles: a novel adsorbent. MethodsX 2018;6:98-106. PMID: 30671353
33. Igwegbe CA, Onyechi PC, Onukwuli OD. Kinetic, isotherm and thermodynamic modelling on the adsorptive removal of malachite green on Dacryodes edulis seeds. J Sci Eng Res 2015;2:23-39. Link
34. Igwegbe CA, Onukwuli OD, Nwabanne JT. Adsorptive removal of vat yellow 4 on activated Mucuna pruriens (velvet bean) seed shells carbon. Asian J Chem Sci 2016;1(1):1-6. Link
35. Igwegbe CA, Mohmmadi L, Ahmadi S, Rahdar A, Khadkhodaiy D, Dehghani R, et al. Modeling of adsorption of methylene blue dye on Ho-$CaWO_4$ nanoparticles using response surface methodology (RSM) and artificial neural network (ANN) techniques. MethodsX 2019;6:1779-97. PMID: 31453114
36. Tarawou T, Wankasi D, Jnr MH. Equilibrium sorption studies of basic blue-9 dye from aqueous

medium using activated carbon produced from water hyacinth (Eichornia Crassipes). J Nepal Chem Soc 2012;29:67-74. Link

37. Nourmoradi H, Daneshfar A, Mazloomi S, Bagheri J, Barati S. Removal of Penicillin G from aqueous solutions by a cationic surfactant modified montmorillonite. MethodsX 2019;6:1967-73. PMID: 31667093
38. Chavoshan S, Khodadadi M, Nasseh N, Hossein Panahi A, Hosseinnejad A. Investigating the efficiency of single-walled and multi-walled carbon nanotubes in removal of penicillin G from aqueous solutions. Environ Health Eng Manag J 2018; 5(4):187-96. Link
39. Rahdar S, Rahdar A, Khodadadi M, Ahmadi S. Error analysis of adsorption isotherm models for penicillin G onto magnesium oxide nanoparticles. Appl Water Sci 2019;9(8):190. Link